7344 *Biochemistry* **2010,** *49,* 7344–7350
DOI: 10.1021/bi100556m

BIOCHEMISTRY
including biophysical chemistry & molecular biology
Article

Pre-Steady State Kinetic Studies of the Fidelity of Nucleotide Incorporation by Yeast DNA Polymerase δ†

Lynne M. Dieckman,‡ Robert E. Johnson,§ Satya Prakash,§ and M. Todd Washington*,‡

‡*Department of Biochemistry, University of Iowa College of Medicine, Iowa City, Iowa 52242-1109, and* §*Department of Biochemistry and Molecular Biology, University of Texas Medical Branch, Galveston, Texas 77555*

Received April 12, 2010; Revised Manuscript Received June 3, 2010

ABSTRACT: Eukaryotic DNA polymerase δ (pol δ) is a member of the B family of polymerases and synthesizes most of the lagging strand during DNA replication. Yeast pol δ is a heterotrimer comprised of three subunits: the catalytic subunit (Pol3) and two accessory subunits (Pol31 and Pol32). Although pol δ is one of the major eukaryotic replicative polymerase, the mechanism by which it incorporates nucleotides is unknown. Here we report both steady state and pre-steady state kinetic studies of the fidelity of pol δ. We found that pol δ incorporates nucleotides with an error frequency of 10^{-4} to 10^{-5}. Furthermore, we showed that for correct versus incorrect nucleotide incorporation, there are significant differences between both pre-steady state kinetic parameters (apparent K_d^{dNTP} and k_{pol}). Somewhat surprisingly, we found that pol δ synthesizes DNA at a slow rate with a k_{pol} of ~1 s^{-1}. We suggest that, unlike its prokaryotic counterparts, pol δ requires replication accessory factors like proliferating cell nuclear antigen to achieve rapid rates of nucleotide incorporation.

Eukaryotic DNA polymerase δ (pol[1] δ), a member of the B family of DNA polymerases, is responsible for synthesizing the bulk of the lagging strand of genomic DNA during normal replication (*1*−*3*). In addition, pol δ participates in nucleotide excision repair, base excision repair, and double-strand break repair (*4*). It also plays an important role in maintaining genome stability, as mutations in pol δ cause an increased frequency of cancer in mice (*5*−*7*) and have been found in cell lines derived from human cancers (*8*, *9*).

Yeast pol δ is a heterotrimer, comprised of three subunits: Pol3 (125 kDa), Pol31 (55 kDa), and Pol32 (40 kDa) (*10*). Pol3 is the catalytic subunit and possesses both DNA polymerase and 3′−5′ exonuclease catalytic activities (*11*, *12*). Pol31 is an accessory subunit that is essential for viability (*13*). By contrast, Pol32 is an accessory subunit that is not essential for viability; however, cells lacking this subunit show defects in DNA replication and repair (*13*). Pol32 also contains the consensus proliferating cell nuclear antigen (PCNA) binding motif, and interactions with PCNA significantly increase the processivity of pol δ (*14*, *15*).

The structure of the Pol3 catalytic subunit of pol δ bound to both DNA and incoming dNTP substrates has recently been determined (*16*). Overall, the structure of the Pol3 subunit resembles that of the bacteriophage RB69 DNA polymerase, another member of the B family of DNA polymerases (*17*, *18*). The catalytic subunit has three domains: an N-terminal domain, an exonuclease domain, and a polymerase domain, which contains palm, fingers, and thumb subdomains. The palm subdomain contains the conserved, acidic residues of the polymerase active site that coordinate the metal ions necessary for catalysis. The fingers subdomain contacts the nascent base pair, and the thumb subdomain contacts the duplex region of the DNA substrate along the minor groove. The DNA polymerase and exonuclease active sites are ~45 Å apart and are located on different domains. In addition, a low-resolution structure of the trimeric form of pol δ shows that the protein has an elongated shape with the Pol31 subunit bridging the Pol3 and Pol32 subunits (*19*).

The general mechanism of nucleotide incorporation by nearly all DNA polymerases examined to date follows the same overall scheme (*20*−*22*). During nonprocessive DNA synthesis, this scheme features four events. First, the polymerase binds the DNA substrate to form the polymerase−DNA binary complex in its preincorporation state. Second, the polymerase−DNA binary complex binds the incoming dNTP to form the polymerase−DNA−dNTP ternary complex. Third, the incoming nucleotide is then incorporated onto the 3′ end of the primer strand of the DNA substrate followed by release of pyrophosphate. This results in the formation of the polymerase−DNA binary complex in its postincorporation state. Fourth, the polymerase dissociates from the DNA substrate. During processive DNA synthesis, the polymerase cycles among the nucleotide binding event, the nucleotide incorporation event, and an additional event in which the polymerase−DNA binary complex in its postincorporation state translocates forward one base pair along the DNA to form the binary complex in its preincorporation state. We note that these events are likely composites of several elementary steps along the reaction pathway, including conformational changes in the polymerase.

Although both the polymerase activity and the proofreading exonuclease activity contribute to the fidelity of DNA synthesis by many DNA polymerases (*23*−*25*), we will focus here on the

†This work was supported by Grant GM081433 from the National Institute of General Medical Sciences to M.T.W. and Grant CA138546 from the National Cancer Institute to S.P.

*To whom correspondence should be addressed: Department of Biochemistry, 4-403 Bowen Science Building, University of Iowa, Iowa City, IA 52242-1109. Phone: (319) 335-7518. Fax: (319) 335-9570. E-mail: todd-washington@uiowa.edu.

[1]Abbreviations: dNTP, deoxynucleoside triphosphate; DTT, dithiothreitol; EDTA, ethylenediaminetetraacetic acid; PCNA, proliferating cell nuclear antigen; pol, polymerase.

 Published on Web 07/28/2010

contribution of the polymerase activity. Polymerases generally prefer to incorporate incoming nucleotides that form correct base pairs with the template base compared to those that form mispairs. This preference often leads to significant differences in the apparent dissociation constant for the incoming dNTP (the apparent K_d^{dNTP}) and in the maximal first-order rate constant for nucleotide incorporation (k_{pol}) for correct versus incorrect nucleotide incorporation. Some polymerases, such as the Klenow fragment of *Escherichia coli* pol I, have significant differences in the k_{pol}, but not in the apparent K_d^{dNTP} (*26*, *27*). By contrast, other polymerases, such as the bacteriophage T7 DNA polymerase, have significant differences in both the apparent K_d^{dNTP} and the k_{pol} (*28*, *29*).

Despite the importance of pol δ in DNA replication and repair and in maintaining genome stability, the mechanism by which it incorporates nucleotides is unknown. Here we report steady state and pre-steady state kinetic studies of yeast pol δ to measure the fidelity of this enzyme and to understand how the kinetics of nucleotide incorporation differs with correct versus incorrect nucleotides. We find that pol δ incorporates most nucleotides with an error frequency of 10^{-4} to 10^{-5}, and we find that there are significant differences between both the apparent K_d^{dNTP} and the k_{pol} for correct versus incorrect nucleotide incorporation. In addition, we find that in the absence of other protein factors, the rate of nucleotide incorporation by pol δ is slower than expected. We suggest that, unlike its prokaryotic counterparts, pol δ requires interactions with other factors like PCNA to achieve the rapid rates of nucleotide incorporation necessary for DNA replication in vivo.

EXPERIMENTAL PROCEDURES

Proteins. *Saccharomyces cerevisiae* pol δ was overexpressed in yeast YRP654 cells carrying plasmids pBJ1244 (containing GST-Pol31), pBJ1180 (containing Pol32), and pBJ1581 (containing FLAG-Pol3 exo$^-$). The protein, which lacked exonuclease activity because it contained two amino acid substitutions in the exonuclease domain (D321A/E323A), was purified as described previously (*30*, *31*). Protein concentrations were determined by the Bio-Rad method and by active site titration, and both methods gave similar results (within 10%).

DNA Substrates. For steady state and pre-steady state kinetic studies, the primer strand was a 32-mer oligodeoxynucleotide with the sequence 5′-GGT AGC CAG CCT CGC ACC CGT CCA ACC AAC TC-3′. The four template strands were 52-mer oligodeoxynucleotides with the sequence 5′-GAC GGC ATT GGA TCG ACC TNG AGT TGG TTG GAC GGG TGC GAG GCT GGC TAC C-3′. In these oligodeoxynucleotides, N represents G, A, T, or C. The primer strand was 5′-^{32}P-end-labeled with T4 polynucleotide kinase and [γ-^{32}P]ATP. The primer and template strands were annealed at 2 μM in 25 mM Tris acetate (pH 7.5) at 90 °C for 2 min and then slowly cooled to room temperature.

Steady State Kinetics. Reactions were performed in 25 mM Tris acetate (pH 7.5), 150 mM sodium acetate, 5 mM magnesium acetate, 1 mM DTT, and 10% glycerol at 30 °C. In the case of correct dNTP incorporation, the 5′-^{32}P-labeled DNA substrate (50 nM) was preincubated with various concentrations of the incoming nucleotide (from 0 to 10 μM), and pol δ (5 nM) was added to the solution to initiate the reaction. Reactions were quenched after 1 min with 10 volumes of formamide loading buffer [80% deionized formamide, 10 mM EDTA (pH 8.0), 1 mg/mL xylene cyanol, and 1 mg/mL bromophenol blue]. The samples were then analyzed on a 15% polyacrylamide sequencing gel containing 8 M urea, and formation of DNA products was quantified by measurement of the intensities of bands using an Instant Imager (Packard). In the case of incorrect dNTP incorporation, the dNTP concentrations used ranged from 0 to 5 mM, and the reactions were quenched after 1 h.

The observed rate of product formation, which was determined by dividing the amount of product formed by the reaction time, was plotted as a function of dNTP concentration. The k_{cat} and K_m values were determined from the best fit of the data to the Michaelis−Menten equation using SigmaPlot 8.0. The error frequency was determined by calculating the ratio of the catalytic efficiency (k_{cat}/K_m) for incorporation of each incorrect dNTP to the sum of the catalytic efficiencies for incorporation of the correct dNTP and three incorrect dNTPs.

Pre-Steady State Kinetics. Reactions were performed under the same buffer conditions as the steady state studies. For correct base pair formation, the reaction times needed to be very short, and thus, the use of a rapid chemical quench flow apparatus (KinTek) was necessary. pol δ (final active concentration of 60 nM) and various concentrations of the DNA substrate (final concentration of 0−150 nM) were preincubated in one syringe of the quench flow. The reactions were initiated by addition of various concentrations of dNTP (0−100 μM) from the other syringe. The quenching solution (0.2 M EDTA) was added to each reaction mixture after short time intervals (0−20 s). The synthesized DNA product was then analyzed using polyacrylamide gel electrophoresis as described above. For incorrect base pair formation, longer reaction times (0−300 s) were used, and thus, experiments could be performed by hand. For these experiments, 150 nM DNA substrate was preincubated with 60 nM pol δ, and the reactions were initiated with addition of various concentrations of nucleotide (0−5 mM). To ensure reproducibility, each set of DNA and dNTP concentrations was repeated multiple times.

For each experiment involving the formation of a correct base pair, the concentration of product formed (P) was plotted as a function of time (t). The observed first-order rate constant of the fast exponential phase (k_{obs}), the amplitude of the fast exponential phase (A), and the velocity of the slow linear phase (v) were determined from the best fit of the data to the burst equation:

$$P = A(1 - e^{-k_{obs}t}) + vt$$

For experiments in which various DNA concentrations were used, the amplitudes of the fast exponential phases (A) were plotted as a function of DNA concentration ([DNA]). The concentration of active pol δ in our protein preparations ([pol δ]) and the dissociation constant for DNA binding (K_d^{DNA}) were determined from the best fit of the data to the quadratic form of the binding equation:

$$A = 0.5(K_d^{DNA} + [\text{pol } \delta] + [\text{DNA}]) - \sqrt{0.25(K_d^{DNA} + [\text{pol } \delta] + [\text{DNA}])^2 - [\text{pol } \delta][\text{DNA}]}$$

For experiments in which various dNTP concentrations were used, the observed first-order rate constants of the fast exponential phases (k_{obs}) were plotted as a function of dNTP concentration ([dNTP]). The apparent dissociation constant for the incoming dNTP (K_d^{dNTP}) and the maximum first-order rate constant for nucleotide incorporation (k_{pol}) were determined

Table 1: Fidelity of pol δ

base pair	k_{cat} (min^{-1})	K_m (μM)	k_{cat}/K_m (μM^{-1} min^{-1})	error frequency[a]
dGTP·G	0.020 ± 0.004	630 ± 350	3.2×10^{-5}	1.6×10^{-5}
dATP·G	0.020 ± 0.002	380 ± 150	5.3×10^{-5}	2.7×10^{-5}
dTTP·G	0.062 ± 0.001	400 ± 30	1.6×10^{-4}	8.0×10^{-5}
dCTP·G	2.7 ± 0.4	1.4 ± 0.6	1.9	N/A[b]
dGTP·A	0.024 ± 0.006	780 ± 440	3.1×10^{-5}	5.2×10^{-5}
dATP·A	0.044 ± 0.008	960 ± 360	4.6×10^{-5}	7.8×10^{-5}
dTTP·A	3.9 ± 1.0	6.6 ± 3.0	0.59	N/A[b]
dCTP·A	0.020 ± 0.002	500 ± 170	4.0×10^{-5}	6.8×10^{-5}
dGTP·T	0.10 ± 0.01	210 ± 20	4.8×10^{-4}	4.5×10^{-4}
dATP·T	2.2 ± 0.2	2.1 ± 0.6	1.0	N/A[b]
dTTP·T	0.022 ± 0.001	410 ± 70	5.4×10^{-5}	5.1×10^{-5}
dCTP·T	0.045 ± 0.002	410 ± 70	1.1×10^{-4}	1.0×10^{-4}
dGTP·C	3.8 ± 0.4	2.5 ± 0.8	1.5	N/A[b]
dATP·C	0.042 ± 0.004	250 ± 100	1.7×10^{-4}	1.1×10^{-4}
dTTP·C	0.11 ± 0.01	660 ± 160	1.7×10^{-4}	1.1×10^{-4}
dCTP·C	N/D[c]	N/D[c]	$< 2 \times 10^{-5}$	$< 1 \times 10^{-5}$

[a]The error frequency is the ratio of the k_{cat}/K_m parameter for incorporation of the incorrect dNTP to the sum of the k_{cat}/K_m parameters for incorporation of the correct dNTP and three incorrect dNTPs. [b]Not applicable. [c]Not detectable.

from the best fit of the data to the rectangular hyperbolic equation:

$$k_{obs} = \frac{k_{pol}[dNTP]}{K_d^{dNTP} + [dNTP]}$$

For each experiment involving the formation of an incorrect base pair, the concentration of product formed was plotted as a function of time. The k_{obs} was determined from the slope of the best fit line divided by the concentration of active pol δ. We conducted kinetic simulations to ensure that the k_{obs} values determined in this manner were valid. The k_{obs} was then plotted as a function of dNTP concentration, and the apparent K_d^{dNTP} and the k_{pol} were determined from the best first of the data to the rectangular hyperbolic equation.

RESULTS

Eukaryotic pol δ synthesizes most of the lagging strand during DNA replication and plays an essential role in several DNA repair pathways. Despite the central role of pol δ in maintaining genome integrity, the kinetic mechanism of nucleotide incorporation by this enzyme is largely unknown. To improve our understanding of the mechanism of this enzyme, we have conducted both steady state kinetic studies and pre-steady state kinetic studies of yeast pol δ. We specifically examined its rate of nucleotide incorporation, its fidelity of nucleotide incorporation, and differences between the kinetics of correct and incorrect nucleotide incorporation. To eliminate any complexities arising from the proofreading exonuclease activity of this enzyme, we have used an exonuclease-deficient mutant form of the protein in all of our experiments.

Fidelity of pol δ. The error frequency of a DNA polymerase is measured by taking the ratio of the catalytic efficiency (k_{cat}/K_m) for incorporation of an incorrect dNTP to the sum of the catalytic efficiencies for incorporation of the correct dNTP and three incorrect dNTPs. Thus, to determine the error frequency of pol δ, we have used steady state kinetics to measure the k_{cat} and K_m values associated with the formation of all 16 possible correct and incorrect base pairs (Table 1). For example, the k_{cat} and K_m for incorporation of the correct dCTP opposite a template G were 2.7 min^{-1} and 1.4 μM, respectively. By contrast, the k_{cat} and K_m for incorporation of the incorrect dGTP opposite a template G were 0.020 min^{-1} and 630 μM, respectively. Consequently, pol δ misincorporates a dGTP opposite a template G with an error frequency of 1.6×10^{-5}. The highest error frequency occurred with dGTP incorporation opposite a template T (4.5×10^{-4}), which is a wobble base pair. The lowest error frequency occurred with incorporation of dCTP opposite a template C ($< 1 \times 10^{-5}$), which was beyond the estimated detection limit for our experiments. The error frequency for all of the other incorrect base pairs was in the range of 10^{-4} to 10^{-5}.

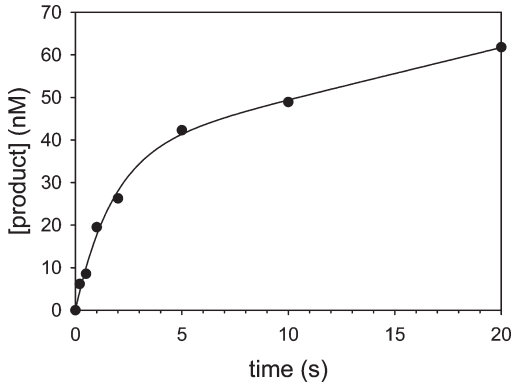

FIGURE 1: Nucleotide incorporation by pol δ displays biphasic kinetics. pol δ (60 nM) was incubated with the DNA substrate (150 nM) and dGTP (50 μM) for various reaction times up to 20 s. The solid line represents the best fit of the data to the burst equation with a k_{obs} for the fast exponential phase equal to 0.58 ± 0.08 s^{-1} and an amplitude of the fast exponential phase equal to 37 ± 3 nM.

pol δ Incorporates Nucleotides with Biphasic Kinetics. While steady state kinetics often provides a convenient means of measuring DNA polymerase fidelity, it provides little information regarding the events occurring at the enzyme active site when correct and incorrect nucleotides are incorporated. Thus, we used pre-steady state kinetics to examine the fidelity of nucleotide incorporation by pol δ. To do this, we first needed to determine whether pol δ exhibited biphasic kinetics (i.e., burst kinetics) under pre-steady state conditions. We preincubated pol δ [final concentration of 60 nM as determined by active site titration (see below)] with the DNA substrate containing a C in the template position (150 nM) in one syringe of a rapid chemical quench flow instrument, and we initiated the reaction by adding dGTP (50 μM) from the second syringe. Figure 1 shows the kinetics of forming a correct G·C base pair in which two phases of nucleotide incorporation are clearly visible. The fast exponential phase represents nucleotide incorporation during the first enzyme turnover, while the slow linear phase represents incorporation during subsequent, steady state turnovers. The rate of incorporation during subsequent turnovers is limited by a slow step in the reaction pathway that occurs after nucleotide incorporation, and this slow step likely represents DNA dissociation, which is generally the case with DNA polymerases. From the best fit of these data to the burst equation, we determined that the observed first-order rate constant (k_{obs}) of the fast phase was equal to 0.58 s^{-1} and the amplitude of the fast phase was equal to 37 nM.

Active Site Titration of pol δ and Determining the K_d^{DNA}. Because pol δ displays biphasic kinetics, we were able to conduct an active site titration to determine the fraction of active pol δ enzyme in our protein preparations and to determine the dissociation constant for DNA binding (K_d^{DNA}). We preincubated pol δ (60 nM) with various concentrations of the DNA

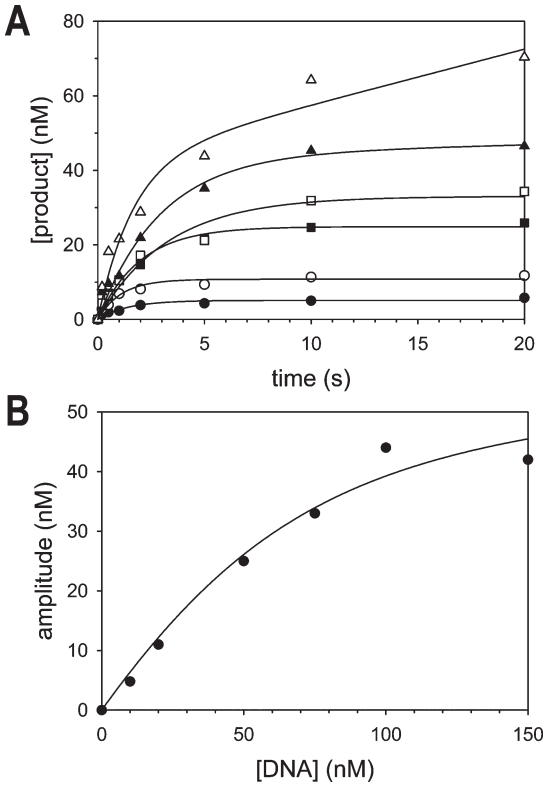

FIGURE 2: Active site titration of pol δ. (A) pol δ (60 nM) was incubated with various concentrations of the DNA substrate [(●) 10, (○) 20, (■) 50, (□) 75, (▲) 100, and (△) 150 nM] and dGTP (50 μM) for various reaction times up to 20 s. The solid lines represent the best fit of the data to the burst equation. (B) The amplitudes of the fast exponential phase were plotted as a function of DNA concentration. The solid line represents the best fit of the data to the quadratic form of the binding equation with a K_d^{DNA} equal to 30 ± 11 nM and a concentration of active pol δ equal to 58 ± 7 nM.

substrate containing a template C (0−150 nM) and initiated the reactions by adding 50 μM dGTP (Figure 2A). The data in each plot were fit using the burst equation, and amplitudes of the fast phases were determined from the best fits. These amplitudes are directly proportional to the amount of active pol δ−DNA complex formed during the preincubation period. Thus, the concentration of active pol δ and the K_d^{DNA} could be determined by plotting the amplitudes as a function of DNA concentration (Figure 2B). From the best fit of these data to the quadratic form of the binding equation, we determined that the concentration of the active pol δ enzyme was equal to 58 nM and that the K_d^{DNA} was equal to 30 nM.

Kinetics of Correct Nucleotide Incorporation by pol δ. To determine the apparent K_d^{dNTP} and the k_{pol} for correct nucleotide incorporation by pol δ, we examined the pre-steady state kinetics of forming a correct G·C base pair. We preincubated pol δ (60 nM) and the DNA substrate with a template C (150 nM) and initiated the reaction by adding various concentrations of dGTP (0−100 μM) (Figure 3A). The data in each plot were fit using the burst equation, and the k_{obs} values of the fast phases were determined from the best fits. These k_{obs} values were plotted as a function of dGTP concentration (Figure 3B). From the best fit of these data to the rectangular hyperbolic equation, we determined that the apparent dissociation constant for nucleotide binding (K_d^{dNTP}) was equal to 36 μM and the maximal first-order rate constant for nucleotide incorporation (k_{pol}) was equal to 1.0 s^{-1}. Table 2 provides the means and standard errors

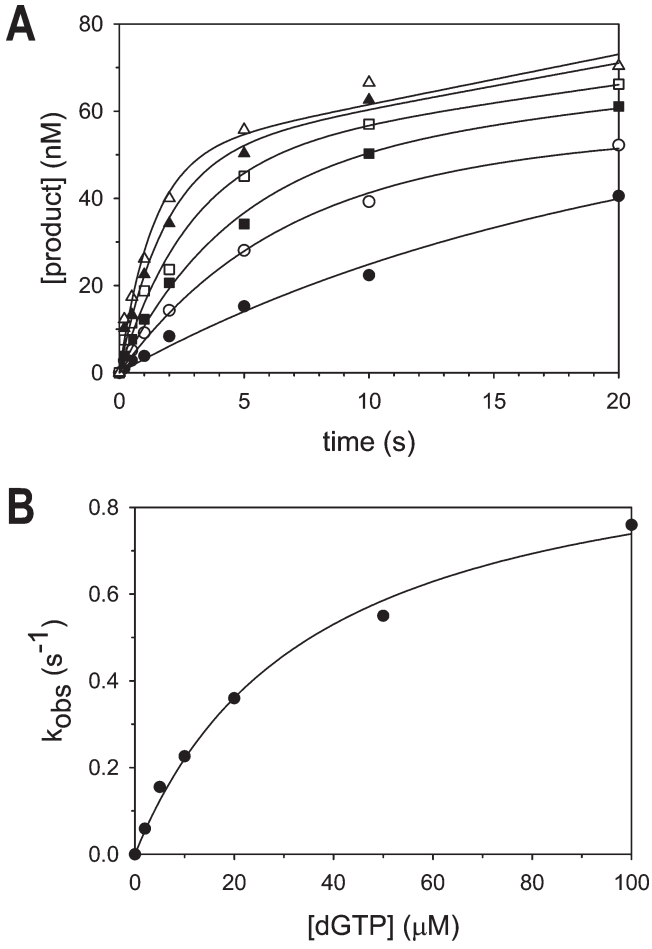

FIGURE 3: Pre-steady state kinetics of correct base pair formation by pol δ. (A) pol δ (60 nM) was incubated with the DNA substrate with a template C residue (150 nM) and various concentrations of dGTP [(●) 2, (○) 5, (■) 10, (□) 20, (▲) 50, and (△) 100 μM] for various reaction times up to 20 s. The solid lines represent the best fit of the data to the burst equation. (B) The k_{obs} values of the fast exponential phases were plotted as a function of dGTP concentration. The solid line represents the best fit of the data to the rectangular hyperbolic equation with an apparent K_d^{dNTP} equal to 36 ± 5 μM and a k_{pol} equal to 1.0 ± 0.1 s^{-1}.

Table 2: Pre-Steady State Kinetics of pol δ

base pair	K_d^{dNTP}[a] (μM)	k_{pol}[a] (s^{-1})	K_d^{dNTP}/K_d^{dNTP}[b]	k_{pol}/k_{pol}[c]
dGTP·G	620 ± 10	0.0023 ± 0.0003	26	400
dGTP·A	330 ± 110	0.0034 ± 0.0013	14	270
dGTP·T	350 ± 30	0.026 ± 0.007	15	36
dGTP·C	24 ± 9	0.93 ± 0.25	N/A	N/A

[a]Values reported here are the means and standard errors from multiple independent experiments. [b]This is the ratio of the apparent K_d^{dNTP} for the incorrect base pair to the apparent K_d^{dNTP} for the correct base pair. [c]This is the ratio of the k_{pol} for the correct base pair to the k_{pol} for the incorrect base pair.

of the apparent K_d^{dNTP} and the k_{pol} values obtained from multiple independent experiments.

Kinetics of Incorrect Nucleotide Incorporation by pol δ. We next examined the pre-steady state kinetics of forming incorrect G·G, G·A, and G·T base pairs. We preincubated pol δ (60 nM) and the DNA substrate with either a template G, template A, or template T (150 nM) and initiated the reaction by addition of various concentrations of dGTP (0−2 mM). Figure 4A shows the kinetics of forming the incorrect G·G base pair.

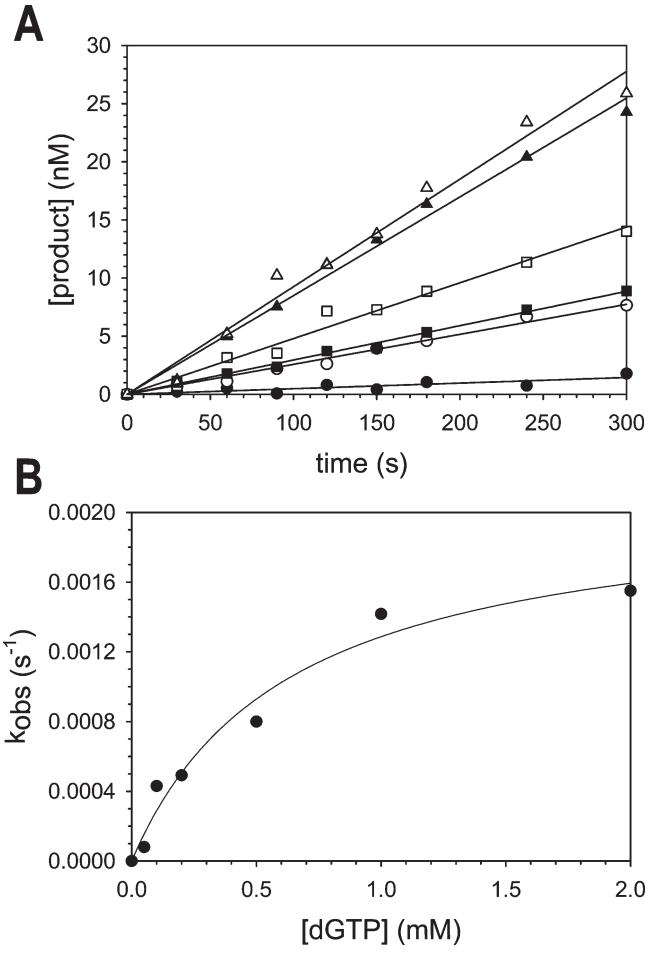

FIGURE 4: Pre-steady state kinetics of incorrect base pair formation by pol δ. (A) pol δ (60 nM) was incubated with the DNA substrate with a template G residue (150 nM) and various concentrations of dGTP [(●) 0.05, (○) 0.1, (■) 0.2, (□) 0.5, (▲) 1, and (△) 2 mM] for various reaction times up to 300 s. The solid line represents the best fit of the data to a linear equation. (B) The k_{obs} values are plotted as a function of dGTP concentration. The solid line represents the best fit of the data to the rectangular hyperbolic equation with an apparent K_d^{dNTP} equal to 630 ± 180 μM and a k_{pol} equal to 0.0021 ± 0.0003 s^{-1}.

The data in each plot were fit to the linear equation, and the k_{obs} values were determined by dividing the slope of the line by the active enzyme concentration. These k_{obs} values were plotted as a function of dGTP concentration (Figure 4B). From the best fit of these data, we determined that the apparent K_d^{dNTP} was equal to 630 μM and the k_{pol} was equal to 0.0021 s^{-1}. The mean and standard error values of the apparent K_d^{dNTP} and k_{pol} parameters for the formation of all three incorrect base pairs obtained from multiple independent experiments are provided in Table 2. The apparent K_d^{dNTP} was approximately 15−30-fold lower in the context of a correct base pair than an incorrect base pair. With the exception of the unusual G·T wobble base pair, the k_{pol} was approximately 250−400-fold faster in the context of a correct base pair than an incorrect base pair. Therefore, there are significant differences between both the apparent K_d^{dNTP} and the k_{pol} for correct versus incorrect nucleotide incorporation.

DISCUSSION

Pre-steady state kinetic studies have been used to examine the mechanisms of a variety of prokaryotic and eukaryotic DNA polymerases. These include eukaryotic repair polymerases like pol β (*32*, *33*), pol λ (*34*), and pol μ (*35*), eukaryotic translesion synthesis polymerases like pol η (*36*, *37*), pol κ (*38*), pol ι (*39*), and Rev1 (*40*), and the mitochondrial polymerase pol γ (*41*). By contrast, very little is known about the mechanisms of the eukaryotic B-family replicative polymerases, which are responsible for synthesizing the leading and lagging strands during genomic DNA replication. Thus, to improve our understanding of the mechanism of eukaryotic pol δ, we examined its fidelity of nucleotide incorporation using steady state and pre-steady state kinetics.

The steady state kinetic analysis reported here shows that the exonuclease-deficient form of yeast pol δ has an error rate of approximately 10^{-4} to 10^{-5}. This is in close agreement with previous studies of the exonuclease-deficient form of yeast pol δ that determined its error rate either from a more limited steady state kinetic analysis or during DNA synthesis across the *lacZ* gene (*42*, *43*). The fidelity of pol δ is similar to the fidelity of the eukaryotic mitochondrial DNA polymerase, pol γ, which has an error rate ranging from 10^{-4} to 10^{-6} (*41*). The fidelity of pol δ is similar to, although in some sequence contexts slightly lower than, the fidelity of the eukaryotic leading strand polymerase, pol ε, which has an error rate of approximately 10^{-4} to 10^{-7} (*44*). By contrast, the fidelity of pol δ is greater than the fidelity of eukaryotic translesion synthesis polymerases such as pol ζ (*45*), pol η (*46*, *47*), pol κ (*48*), and pol ι (*45*, *49*, *50*), which have error rates as high as 10^{1} for pol ι and as low as 10^{-4} for pol ζ and pol κ.

The kinetics of correct base pair formation by pol δ reported here allows for a direct comparison of this enzyme with other DNA polymerases. The apparent K_d^{dNTP} of pol δ, for example, is ~20 μM, which is similar (i.e., within a factor of 5) to the apparent K_d^{dNTP} reported for replicative DNA polymerases from bacteriophage, such as the T7 DNA polymerase (*28*), the T4 polymerase (*51*), and the RB69 DNA polymerase (*52*). By contrast, the k_{pol} of pol δ is ~1 s^{-1}, which is at least 200-fold slower than those reported for these bacteriophage replicative polymerases (*28*, *51*, *52*). This k_{pol} value is, in fact, more typical of some of the eukaryotic DNA repair polymerases of the X family, such as pol β (*32*), pol λ (*34*), and pol μ (*35*) and eukaryotic translesion synthesis polymerases of the Y family, such as pol η (*36*), pol ι (*39*), and pol κ (*38*). It is important to point out that this low k_{pol} is not due to inactive pol δ in our protein preparations. This low k_{pol} was observed with multiple protein preparations, and active site titrations showed that nearly all of the pol δ in our preparations was active. This low k_{pol} value, however, is similar to the k_{pol} reported for calf thymus pol δ, which was ~6 s^{-1} (*53*). Therefore, it seems that eukaryotic pol δ may be intrinsically slow at nucleotide incorporation in the absence of replication accessory factors when compared to replicative polymerases from simpler bacteriophage systems.

We believe that the interactions with other factors, such as PCNA (the sliding clamp processivity factor), are required for pol δ to achieve the rapid rate of DNA synthesis necessary for DNA replication in vivo. Support for this comes from the fact that PCNA was shown to increase the k_{pol} of calf thymus pol δ by more than 3-fold (*53*). In that study, however, PCNA was inefficiently loaded onto the DNA, because replication factor C (the clamp loader) was not present and the ends of the DNA were not blocked to prevent PCNA from sliding off the substrate. Thus, when loaded onto DNA by RFC, PCNA would enhance the rate of nucleotide incorporation by calf thymus pol δ to a greater degree than what has been previously reported. Moreover, we note that data presented by Chen et al. (*54*) show that PCNA dramatically stimulates the nucleotide incorporation

activity of *Schizosaccharomyces pombe* pol δ and not merely its processivity.

A comparison of the kinetics of correct and incorrect nucleotide incorporation reported here shows that the fidelity of DNA synthesis by pol δ results in significant differences between both the apparent K_d^{dNTP} and the k_{pol} for correct versus incorrect nucleotide incorporation. For example, the apparent K_d^{dNTP} is 26-fold tighter when the base pair is correct (G·C) than when it is incorrect (G·G), and the incoming nucleotide is added to the 3′ end of the primer strand 400-fold faster when the base pair is correct than when it is incorrect. One must be careful, however, about interpreting these differences in terms of the elementary steps along the reaction pathway. Recent studies have called into question the assumption that the apparent K_d^{dNTP} reflects the ground state binding affinity of the incoming dNTP (*55*, *56*). Moreover, there is significant debate in the literature regarding the contributions of the chemical step of phosphodiester bond formation and a conformational change step (both in its forward direction and in its reverse direction) that precedes the chemical step (*57*−*59*). Thus, proper interpretation of the changes in the apparent K_d^{dNTP} and k_{pol} in terms of the elementary steps along the reaction pathway and how these steps contribute to the fidelity of pol δ will require a complete analysis of all steps, including any conformational change steps.

Nevertheless, with respect to these significant differences in both the apparent K_d^{dNTP} and the k_{pol} for correct versus incorrect nucleotide incorporation, pol δ resembles other replicative DNA polymerases, including the bacteriophage T7 DNA polymerase (*28*, *29*), the *Sulfolobus solfataricus* pol B1 (*60*), and human mitochondrial pol γ (*41*). This is in contrast to some nonreplicative polymerases, including repair polymerases like *E. coli* pol I (Klenow fragment) (*26*, *27*) and translesion synthesis polymerases like *S. solfactaricus* Dpo4 (*61*) and eukaryotic pol η (*36*, *37*). Many of these nonreplicative polymerases have significant changes only in the k_{pol} for correct versus incorrect nucleotide incorporation. This suggests a general trend across both prokaryotes and eukaryotes whereby replicative polymerases tend to have significant differences in both the apparent K_d^{dNTP} and k_{pol} and nonreplicative (i.e., repair and translesion synthesis) polymerases tend to have significant differences in the k_{pol}.

The X-ray crystal structure of the catalytic subunit of yeast pol δ has recently been determined (*16*), which to the best of our knowledge is the only available structure for a eukaryotic, replicative DNA polymerase. Moreover, a low-resolution structure has been determined for the complex containing all three subunits of yeast pol δ (*19*). These structures make yeast pol δ the ideal system for examining the structure−function relationship in a eukaryotic B-family polymerase. The kinetics of pol δ reported here provides an excellent platform for these studies. It also provides a basis for understanding the impact of the cancer-causing mutant forms of this protein as well as understanding the role of replication accessory factors, such as PCNA, in promoting its DNA synthesis activity.

ACKNOWLEDGMENT

We thank Christine Kondratick, Bret Freudenthal, John Pryor, and Louise Prakash for valuable discussions.

REFERENCES

1. Burgers, P. M. J. (2009) Polymerase Dynamics at the Eukaryotic DNA Replication Fork. *J. Biol. Chem. 284*, 4041–4045.
2. Kunkel, T. A., and Burgers, P. M. (2008) Dividing the workload at a eukaryotic replication fork. *Trends Cell Biol. 18*, 521–527.
3. McElhinny, S. A. N., Gordenin, D. A., Stith, C. M., Burgers, P. M. J., and Kunkel, T. A. (2008) Division of labor at the eukaryotic replication fork. *Mol. Cell 30*, 137–144.
4. Shcherbakova, P. V., Bebenek, K., and Kunkel, T. A. (2003) Functions of eukaryotic DNA polymerases. *Sci. Aging Knowledge Environ. 2003*, RE3.
5. Goldsby, R. E., Hays, L. E., Chen, X., Olmsted, E. A., Slayton, W. B., Spangrude, G. J., and Preston, B. D. (2002) High incidence of epithelial cancers in mice deficient for DNA polymerase δ proofreading. *Proc. Natl. Acad. Sci. U.S.A. 99*, 15560–15565.
6. Goldsby, R. E., Lawrence, N. A., Hays, L. E., Olmsted, E. A., Chen, X., Singh, M., and Preston, B. D. (2001) Defective DNA polymerase-δ proofreading causes cancer susceptibility in mice. *Nat. Med. 7*, 638–639.
7. Venkatesan, R. N., Treuting, P. M., Fuller, E. D., Goldsby, R. E., Norwood, T. H., Gooley, T. A., Ladiges, W. C., Preston, B. D., and Loeb, L. A. (2007) Mutation at the polymerase active site of mouse DNA polymerase δ increases genomic instability and accelerates tumorigenesis. *Mol. Cell. Biol. 27*, 7669–7682.
8. Flohr, T., Dai, J. C., Buttner, J., Popanda, O., Hagmuller, E., and Thielmann, H. W. (1999) Detection of mutations in the DNA polymerase δ gene of human sporadic colorectal cancers and colon cancer cell lines. *Int. J. Cancer 80*, 919–929.
9. Dacosta, L. T., Liu, B., Eldeiry, W. S., Hamilton, S. R., Kinzler, K. W., Vogelstein, B., Markowitz, S., Willson, J. K. V., Delachapelle, A., Downey, K. M., and So, A. G. (1995) Polymerase-δ Variants in Rer Colorectal Tumors. *Nat. Genet. 9*, 10–11.
10. Johansson, E., Majka, J., and Burgers, P. M. J. (2001) Structure of DNA polymerase δ from *Saccharomyces cerevisiae*. *J. Biol. Chem. 276*, 43824–43828.
11. Sitney, K. C., Budd, M. E., and Campbell, J. L. (1989) DNA Polymerase-III, a second Essential DNA-Polymerase, Is Encoded by the *S. cerevisiae Cdc2* Gene. *Cell 56*, 599–605.
12. Boulet, A., Simon, M., Faye, G., Bauer, G. A., and Burgers, P. M. J. (1989) Structure and Function of the *Saccharomyces cerevisiae Cdc2* Gene Encoding the Large Subunit of DNA Polymerase-III. *EMBO J. 8*, 1849–1854.
13. Gerik, K. J., Li, X. Y., Pautz, A., and Burgers, P. M. J. (1998) Characterization of the two small subunits of *Saccharomyces cerevisiae* DNA polymerase δ. *J. Biol. Chem. 273*, 19747–19755.
14. Burgers, P. M. J., and Gerik, K. J. (1998) Structure and processivity of two forms of *Saccharomyces cerevisiae* DNA polymerase δ. *J. Biol. Chem. 273*, 19756–19762.
15. Johansson, E., Garg, P., and Burgers, P. M. J. (2004) The pol32 subunit of DNA polymerase δ contains separable domains for processive replication and proliferating cell nuclear antigen (PCNA) binding. *J. Biol. Chem. 279*, 1907–1915.
16. Swan, M. K., Johnson, R. E., Prakash, L., Prakash, S., and Aggarwal, A. K. (2009) Structural basis of high-fidelity DNA synthesis by yeast DNA polymerase delta. *Nat. Struct. Mol. Biol. 16*, 979–983.
17. Franklin, M. C., Wang, J. M., and Steitz, T. A. (2001) Structure of the replicating complex of a pol α family DNA polymerase. *Cell 105*, 657–667.
18. Wang, J., Sattar, A., Wang, C. C., Karam, J. D., Konigsberg, W. H., and Steitz, T. A. (1997) Crystal structure of a pol α family replication DNA polymerase from bacteriophage RB69. *Cell 89*, 1087–1099.
19. Jain, R., Hammel, M., Johnson, R. E., Prakash, L., Prakash, S., and Aggarwal, A. K. (2009) Structural Insights into Yeast DNA Polymerase δ by Small Angle X-ray Scattering. *J. Mol. Biol. 394*, 377–382.
20. Rothwell, P. J., and Waksman, G. (2005) Structure and mechanism of DNA polymerases. *Adv. Protein Chem. 71*, 401–440.
21. Johnson, K. A. (1995) Rapid Quench Kinetic-Analysis of Polymerases, Adenosine-Triphosphatases, and Enzyme Intermediates. *Methods Enzymol. 249*, 38–61.
22. Johnson, K. A. (2010) The kinetic and chemical mechanism of high-fidelity DNA polymerases. *Biochim. Biophys. Acta 1804*, 1041–1048.
23. Kunkel, T. A., and Bebenek, R. (2000) DNA replication fidelity. *Annu. Rev. Biochem. 69*, 497–529.
24. Kunkel, T. A. (2004) DNA replication fidelity. *J. Biol. Chem. 279*, 16895–16898.
25. McCulloch, S. D., and Kunkel, T. A. (2008) The fidelity of DNA synthesis by eukaryotic replicative and translesion synthesis polymerases. *Cell Res. 18*, 148–161.
26. Kuchta, R. D., Benkovic, P., and Benkovic, S. J. (1988) Kinetic Mechanism Whereby DNA-Polymerase-I (Klenow) Replicates DNA with High Fidelity. *Biochemistry 27*, 6716–6725.

27. Kuchta, R. D., Mizrahi, V., Benkovic, P. A., Johnson, K. A., and Benkovic, S. J. (1987) Kinetic Mechanism of DNA-Polymerase-I (Klenow). *Biochemistry 26*, 8410–8417.
28. Patel, S. S., Wong, I., and Johnson, K. A. (1991) Pre-Steady-State Kinetic-Analysis of Processive DNA-Replication Including Complete Characterization of an Exonuclease-Deficient Mutant. *Biochemistry 30*, 511–525.
29. Wong, I., Patel, S. S., and Johnson, K. A. (1991) An Induced-Fit Kinetic Mechanism for DNA-Replication Fidelity: Direct Measurement by Single-Turnover Kinetics. *Biochemistry 30*, 526–537.
30. Zhuang, Z. H., Johnson, R. E., Haracska, L., Prakash, L., Prakash, S., and Benkovic, S. J. (2008) Regulation of polymerase exchange between Pol η and Pol δ by monoubiquitination of PCNA and the movement of DNA polymerase holoenzyme. *Proc. Natl. Acad. Sci. U.S.A. 105*, 5361–5366.
31. Johnson, R. E., Prakash, L., and Prakash, S. (2006) Yeast and human translesion DNA synthesis polymerases: Expression, purification, and biochemical characterization. *Methods Enzymol. 408*, 390–407.
32. Ahn, J., Werneburg, B. G., and Tsai, M. D. (1997) DNA polymerase β: Structure-fidelity relationship from pre-steady-state kinetic analyses of all possible correct and incorrect base pairs for wild type and R283A mutant. *Biochemistry 36*, 1100–1107.
33. Werneburg, B. G., Ahn, J., Zhong, X. J., Hondal, R. J., Kraynov, V. S., and Tsai, M. D. (1996) DNA polymerase β: Pre-steady-state kinetic analysis and roles of arginine-283 in catalysis and fidelity. *Biochemistry 35*, 7041–7050.
34. Fiala, K. A., Abdel-Gawad, W., and Suo, Z. (2004) Pre-steady-state kinetic studies of the fidelity and mechanism of polymerization catalyzed by truncated human DNA polymerase λ. *Biochemistry 43*, 6751–6762.
35. Roettger, M. P., Fiala, K. A., Sompalli, S., Dong, Y. X., and Suo, Z. C. (2004) Pre-steady-state kinetic studies of the fidelity of human DNA polymerase μ. *Biochemistry 43*, 13827–13838.
36. Washington, M. T., Prakash, L., Prakash, S., and Yeast, D. N. A. (2001) polymerase η utilizes an induced-fit mechanism of nucleotide incorporation. *Cell 107*, 917–927.
37. Washington, M. T., Johnson, R. E., Prakash, L., and Prakash, S. (2003) The mechanism of nucleotide incorporation by human DNA polymerase η differs from that of the yeast enzyme. *Mol. Cell. Biol. 23*, 8316–8322.
38. Carlson, K. D., Johnson, R. E., Prakash, L., Prakash, S., and Washington, M. T. (2006) Human DNA polymerase κ forms nonproductive complexes with matched primer termini but not with mismatched primer termini. *Proc. Natl. Acad. Sci. U.S.A. 103*, 15776–15781.
39. Washington, M. T., Johnson, R. E., Prakash, L., Prakash, S., and Human, D. N. A. (2004) polymerase ι utilizes different nucleotide incorporation mechanisms dependent upon the template base. *Mol. Cell. Biol. 24*, 936–943.
40. Howell, C. A., Prakash, S., and Washington, M. T. (2007) Pre-steady-state kinetic studies of protein-template-directed nucleotide incorporation by the yeast rev1 protein. *Biochemistry 46*, 13451–13459.
41. Johnson, A. A., and Johnson, K. A. (2001) Fidelity of nucleotide incorporation by human mitochondrial DNA polymerase. *J. Biol. Chem. 276*, 38090–38096.
42. Fortune, J. M., Pavlov, Y. I., Welch, C. M., Johansson, E., Burgers, P. M. J., and Kunkel, T. A. (2005) *Saccharomyces cerevisiae* DNA polymerase δ: High fidelity for base substitutions but lower fidelity for single- and multi-base deletions. *J. Biol. Chem. 280*, 29980–29987.
43. Hashimoto, K., Shimizu, K., Nakashima, N., and Sugino, A. (2003) Fidelity of DNA polymerase δ holoenzyme from *Saccharomyces cerevisiae*: The sliding clamp proliferating cell nuclear antigen decreases its fidelity. *Biochemistry 42*, 14207–14213.
44. Shimizu, K., Hashimoto, K., Kirchner, J. M., Nakai, W., Nishikawa, H., Resnick, M. A., and Sugino, A. (2002) Fidelity of DNA polymerase ε holoenzyme from budding yeast *Saccharomyces cerevisiae*. *J. Biol. Chem. 277*, 37422–37429.
45. Johnson, R. E., Washington, M. T., Haracska, L., Prakash, S., and Prakash, L. (2000) Eukaryotic polymerases ι and ζ act sequentially to bypass DNA lesions. *Nature 406*, 1015–1019.
46. Johnson, R. E., Washington, M. T., Prakash, S., and Prakash, L. (2000) Fidelity of human DNA polymerase η. *J. Biol. Chem. 275*, 7447–7450.
47. Washington, M. T., Johnson, R. E., Prakash, S., and Prakash, L. (1999) Fidelity and processivity of *Saccharomyces cerevisiae* DNA polymerase η. *J. Biol. Chem. 274*, 36835–36838.
48. Johnson, R. E., Prakash, S., and Prakash, L. (2000) The human DINB1 gene encodes the DNA polymerase Pol θ. *Proc. Natl. Acad. Sci. U.S.A. 97*, 3838–3843.
49. Tissier, A., McDonald, J. P., Frank, E. G., and Woodgate, R. (2000) Pol ι a remarkably error-prone human DNA polymerase. *Genes Dev. 14*, 1642–1650.
50. Zhang, Y. B., Yuan, F. H., Wu, X. H., and Wang, Z. G. (2000) Preferential incorporation of G opposite template T by the low-fidelity human DNA polymerase ι. *Mol. Cell. Biol. 20*, 7099–7108.
51. Capson, T. L., Peliska, J. A., Kaboord, B. F., Frey, M. W., Lively, C., Dahlberg, M., and Benkovic, S. J. (1992) Kinetic Characterization of the Polymerase and Exonuclease Activities of the Gene-43 Protein of Bacteriophage-T4. *Biochemistry 31*, 10984–10994.
52. Yang, G. W., Franklin, M., Li, J., Lin, T. C., and Konigsberg, W. (2002) A conserved Tyr residue is required for sugar selectivity in a pol α DNA polymerase. *Biochemistry 41*, 10256–10261.
53. Einolf, H. J., and Guengerich, F. P. (2000) Kinetic analysis of nucleotide incorporation by mammalian DNA polymerase δ. *J. Biol. Chem. 275*, 16316–16322.
54. Chen, X. L., Zuo, S. J., Kelman, Z., O'Donnell, M., Hurwitz, J., and Goodman, M. J. (2000) Fidelity of eucaryotic DNA polymerase δ holoenzyme from *Schizosaccharomyces pombe*. *J. Biol. Chem. 275*, 17677–17682.
55. Tsai, Y. C., and Johnson, K. A. (2006) A new paradigm for DNA polymerase specificity. *Biochemistry 45*, 9675–9687.
56. Kellinger, M. W., and Johnson, K. A. (2010) Nucleotide-dependent conformational change governs specificity and analog discrimination by HIV reverse transcriptase. *Proc. Natl. Acad. Sci. U.S.A. 107*, 7734–7739.
57. Bakhtina, M., Roettger, M. P., and Tsai, M. D. (2009) Contribution of the Reverse Rate of the Conformational Step to Polymerise β Fidelity. *Biochemistry 48*, 3197–3208.
58. Roettger, M. P., Bakhtina, M., and Tsai, M. D. (2008) Mismatched and matched dNTP incorporation by DNA polymerase β proceed via analogous kinetic pathways. *Biochemistry 47*, 9718–9727.
59. Bakhtina, M., Roettger, M. P., Kumar, S., and Tsai, M. D. (2007) A unified kinetic mechanism applicable to multiple DNA polymerases. *Biochemistry 46*, 5463–5472.
60. Zhang, L. K., Brown, J. A., Newmister, S. A., and Suo, Z. C. (2009) Polymerization Fidelity of a Replicative DNA Polymerase from the Hyperthermophilic Archaeon *Sulfolobus solfataricus* P2. *Biochemistry 48*, 7492–7501.
61. Fiala, K. A., and Suo, Z. (2004) Pre-steady-state kinetic studies of the fidelity of *Sulfolobus solfataricus* P2 DNA polymerase IV. *Biochemistry 43*, 2106–2115.